DNA Actuator

DOI: 10.1002/ange.201007642

A DNA Tile Actuator with Eleven Discrete States**

*Zhao Zhang, Eva M. Olsen, Mille Kryger, Niels V. Voigt, Thomas Tørring, Eda Gültekin, Morten Nielsen, Reza MohammadZadegan, Ebbe S. Andersen, Morten M. Nielsen, Jørgen Kjems, Victoria Birkedal, and Kurt V. Gothelf**

The dynamic nature of DNA hybridization has been utilized to design nanostructures that can switch between geometrically well-defined states.[1] Seeman and co-workers pioneered the design of DNA devices that could reversibly switch between two different states.[2] One of these structures was recently applied as a DNA robot arm in a nanoscale assembly line.[3] Extension and contraction of nanostructures between 2 or 3 states have been executed by using DNA hairpins.[4] Herein we report on a novel DNA actuator design that undergoes a sliding type motion between 11 discrete states. The actuator can be locked in any of the 2 nucleotide-spaced states, as shown by fluorescence resonance energy transfer (FRET) and by the strict control of a chemical reaction. By strand displacement reactions, the actuator can be switched between the states. The actuator operates as a nanoscale extendable arm and the integration of one or more actuators in larger nanostructures holds promise for designing more sophisticated dynamic DNA devices.

Our actuator design is based on the principles of the Holliday junction, which plays a pertinent role in genetic recombination.[5] The Holliday junction is a mobile four-way junction of homologous sequences that allows the junction to slide along the DNA.[6] Nevertheless, most artificial dynamic DNA designs, such as motors,[7] walkers,[8] and machines,[9] are based on other switching mechanisms. The only exception is the double-crossover tile reported by Seeman and co-workers in 2000, which allowed irreversible migration from one partly mismatched state to another fully matched state.[10]

The DNA actuator presented herein structurally resembles the double-crossover tile (Figure 1a), which is one of the most common motifs in DNA nanostructures.[11] Our actuator is composed of two pistons A and B, a roller R, and in the locked states, two identical lock strands (Figure 1b–d). Four 11-nucleotide regions in the two piston strands are identical while the central 21-nucleotide region of each of the pistons is unique. The roller strand R contains two 11-nucleotide regions that are complementary to either of the two peripheral red regions on A and B. The sequence symmetry around the two half crossovers allows the actuator to migrate along the horizontal direction parallel to the pistons. In the unlocked state (Figure 1b and c), the preferred state of the actuator is unknown and the system may be in a dynamic balance between the states. To force the actuator to adopt specific states, a series of 11 lock strands (Ln) are used; each lock can hybridize with a part of both pistons. As opposed to Holliday junctions and DX tiles, the half crossovers of the lock strands are here positioned 11 nucleotides or one helical turn away from the two half crossovers of the roller. Since there is no sequence similarity around the half crossover of the locks, the migration is arrested and the actuator is locked

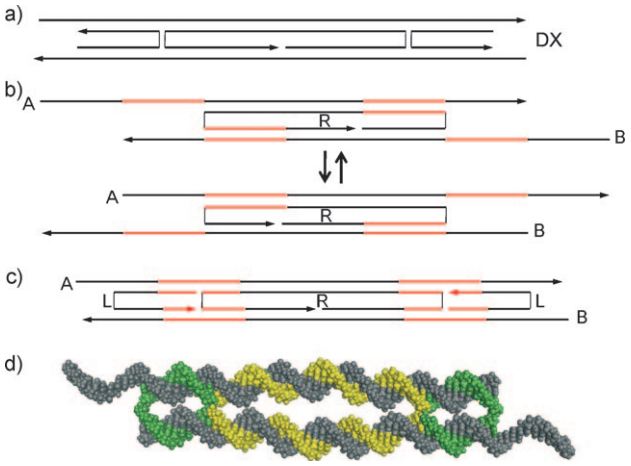

Figure 1. Schematic illustration and 3D model of a DNA actuator. a) Classic design of the DX tile inspired by the Holliday junction. b) Three DNA strands, piston A (A), piston B (B), and roller (R), are annealed to form the core of the actuator. c) A lock strand (L) is used to fix the position of the metastable ABR complex into a specific state. d) A full-atom model of the actuator. The maximum distance between centers of two helices is chosen as 3 nm.

[*] Dr. Z. Zhang,[+] E. M. Olsen,[+] M. Kryger, N. V. Voigt, T. Tørring, E. Gültekin, M. Nielsen, R. MohammadZadegan, Dr. E. S. Andersen, M. M. Nielsen, Prof. J. Kjems, Dr. V. Birkedal, Prof. K. V. Gothelf
Center for DNA Nanotechnology (CDNA) at the Interdisciplinary Nanoscience Center (iNANO), Aarhus University
8000 Aarhus C (Denmark)
Fax: (+45) 8619-6199
E-mail: kvg@chem.au.dk

Dr. Z. Zhang,[+] E. M. Olsen,[+] M. Kryger, N. V. Voigt, T. Tørring, E. Gültekin, M. Nielsen, Prof. K. V. Gothelf
Department of Chemistry, Aarhus University (Denmark)

R. MohammadZadegan, Dr. E. S. Andersen, M. M. Nielsen, Prof. J. Kjems
Department of Molecular Biology, Aarhus University (Denmark)

Dr. V. Birkedal
iNANO Center, Aarhus University (Denmark)

[+] These authors contributed equally to this work.

[**] This work was supported by grants from the Danish National Research Foundation to the CDNA Center, the Danish Research Agency through support to the iNANO Center, and the Danish Council for Independent Research.

Supporting information for this article is available on the WWW under http://dx.doi.org/10.1002/anie.201007642.

in a specific state. An atomic model of the DNA actuator was constructed (Figure 1 d). Earlier studies have shown that the helices bend away from each other between two crossovers because of electrostatic repulsion and entropic effects.[11,12] In the model presented here we have assumed a maximum distance of 3 nm between the centers of the two helices.[12–13]

The sequences of the open ABR actuator are shown in Figure 2 a, along with the actuator locked in three different

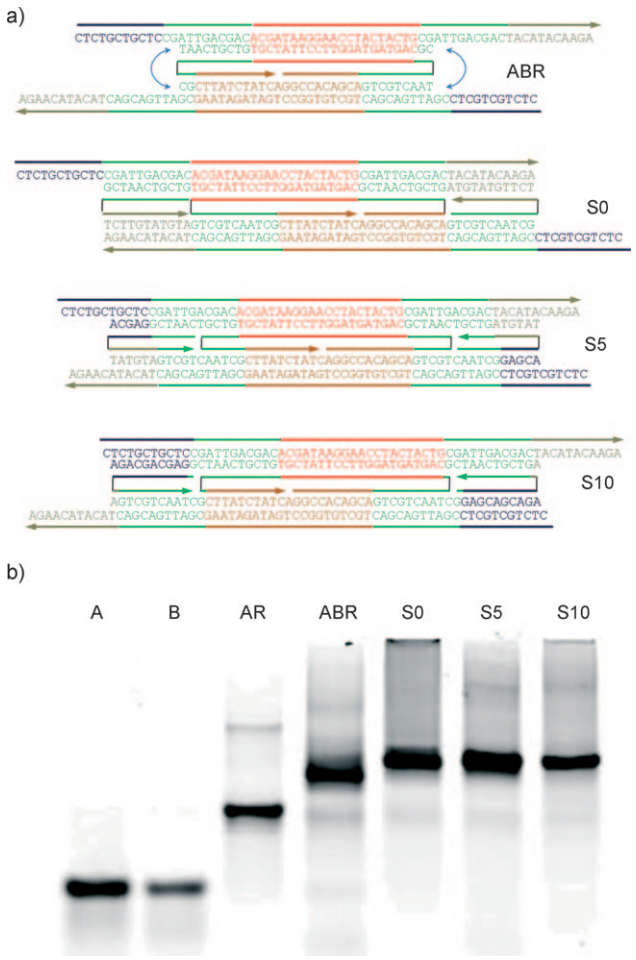

Figure 2. a) The actual sequences used in the reported experiments. As shown here in distinct colors, three lock strands, L0, L5, and L10, lock the actuator in state 0 (S0), state 5 (S5), and state 10 (S10) respectively. Number of nucleotides in each strand: A = B = 65, R = 64, Ln = 22 (see section S1 in the Supporting Information for sequence details). b) A 7.5 % native PAGE that shows the actuator in different states. The clear and single band in each lane indicates the high assembly efficiency.

states, state 0 (S0), state 5 (S5), and state 10 (S10), using two equivalents of locks L0, L5, and L10, respectively. We define S0 as the position where the upper piston A is shifted to the far left position and the lower piston B is shifted to the far right position. Our actuator is assembled by mixing stoichiometric quantities of the two pistons and the roller in TAE/Mg^{2+} buffer.[14] The flanking homologous region has 11 bases and hence 11 different locks can be designed and applied to select any of the states defined as 0, 1, 2 etc. to 10. Between two succeeding steps, the pistons undergo a 2-nucleotide (6.8 Å) relative displacement. When the actuator is sliding, the two DNA helices rotate in opposite directions, unwinding and winding the pistons at each of the roller half crossovers.

Fluorophores were inserted at strategic positions in piston A and B to characterize the structural changes of the DNA actuator through the 11 different states by FRET.[15] The FRET signal is in theory proportional to the inverse sixth power of the distance between the two fluorophores, thus providing detailed information on structural changes.

In the first example, piston A is conjugated to Alexa647 and piston B to Cy3B. For this pair, both fluorophores are located in the middle of the complex in state S0, that is, they are both placed 16 nucleotides, or one and a half helical turns, from the right-hand half crossover of the roller (Figure 3 a–c). Hence, in S0 the two fluorophores are both in the same horizontal position and both inside the complex. In state S1 (complex formed with L1) the fluorophores are each shifted one nucleotide in opposite directions in the horizontal direction (piston A to the right and piston B to the left) and this separation increases in the following states S2 to S10. In the vertical direction, the fluorophores are gradually moving from the inside of the structure in S0 to the outside of the helices and the maximal vertical separation is obtained in states S5 and S6. Theoretical models with bent helices were constructed by energy minimization techniques (for detailed methods see section S3 in the Supporting Information) and theoretical FRET values were calculated. Measurement of FRET values for each state S0–S10 was carried out both in solution using a fluorometer and by FRET analysis of the product band in a native polyacrylamide gel electrophoresis (PAGE) gel using a Typhoon scanner (see the Supporting Information, Figure S10). The measured FRET efficiencies are shown in Figure 3 b (see section S4 in the Supporting Information).

In the second example, the fluorophores are located 10 nucleotides apart in S0 (Figure 3 d), that is, the fluorophore on A (Alexa555) is located 21 nucleotides from the right-hand half crossover of the roller and the fluorophore on B (Alexa647) is located 11 nucleotides from the right half crossover of the roller. Hence, from state S0 to state S5, the fluorophores will approach each other in both the vertical and the horizontal direction and will intercross in S5. From S5 to S10 the fluorophores will move apart in a similar reverse track. A third design where both dyes are 6 nucleotides apart, or half a helical turn, from the right-hand half crossover of the roller in S0, is shown in Figure S8.

In general, the curves from the experimental and theoretical FRET values show similar overall shapes (Figure 3 b,c,e,f), thus indicating that the relative positions of the fluorophores are shifting as expected between the different states of the actuator. For calculation of the theoretical FRET values, a maximum separation of the center of the two helices of 3 nm distance was chosen after a detailed theoretical bending study. This study was performed by varying the distance between the two helices followed by energy minimization (see section S3 in the Supporting Information). The relative decrease in bulk FRET efficiency in state S0 in Figure 3 b and state S5 in Figure 3 e appears for the states

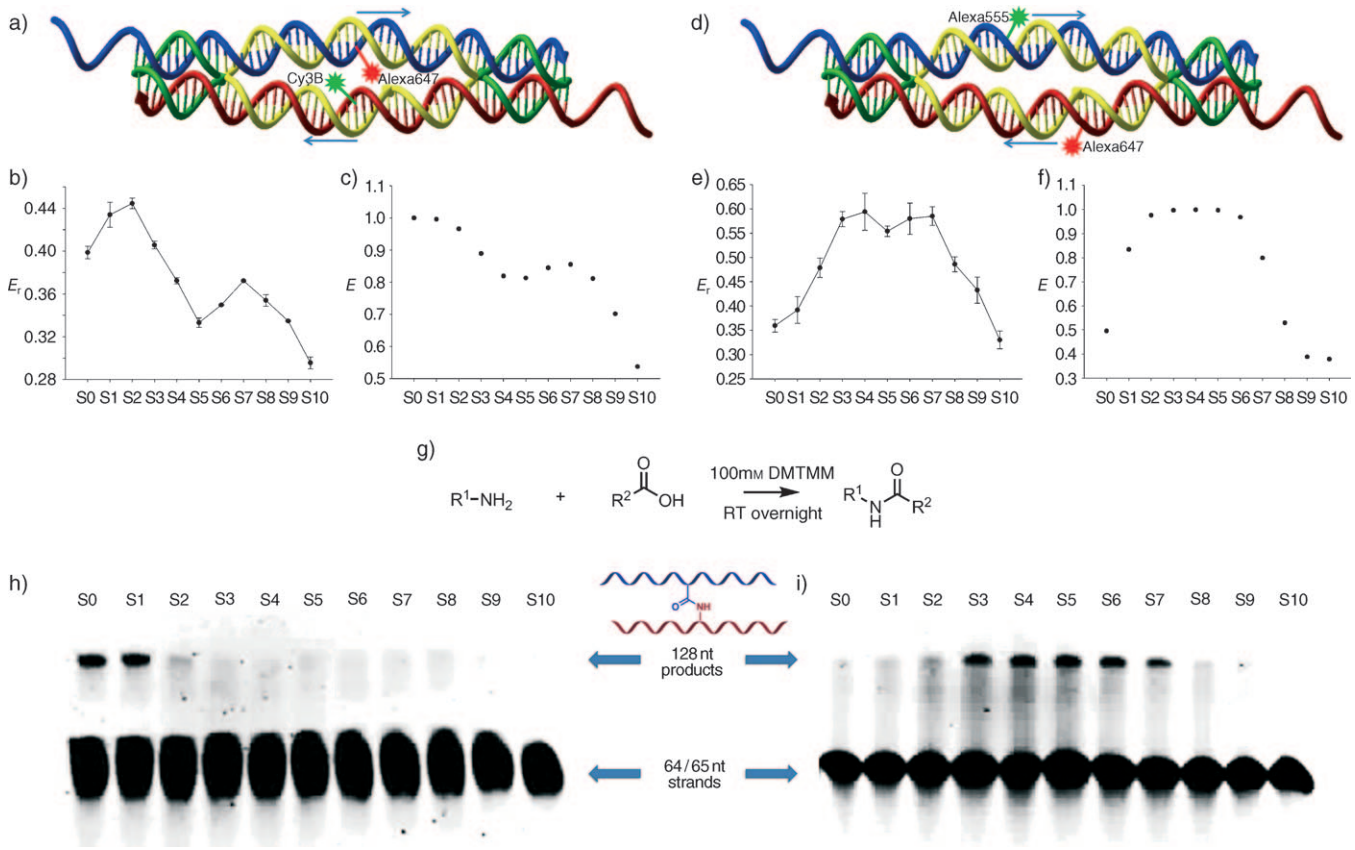

Figure 3. FRET values and chemical reactions for the 11 different states of the actuator. a) For an actuator where the dyes Alexa647 and Cy3B are each positioned on the pistons 16 nucleotides from the right-hand half crossover of the roller in S0, b) experimental relative FRET efficiency values, c) theoretical FRET values obtained using R0 = 4.9 nm, d) actuator where the dyes Alexa555 and Alexa647 are each positioned on the pistons 21 nucleotides and 11 nucleotides from the right-hand half crossover of the roller in S0, e) experimental relative FRET values, f) theoretical FRET values using R0 = 6.8 nm. g) The chemical coupling reaction between the amine and carboxylic acid groups in the two pistons is mediated by the activator 4-(4,6-dimethoxy-1,3,5-triazin-2-yl)-4-methylmorpholinium chloride (DMTMM) and results in the formation of an amide group. Denaturing PAGE analysis of the chemical reactions of the actuator in the 11 different states for the amine and carboxylic acid groups placed as the dyes in h) the design in (a) and i) the design in (d). nt = nucleotides.

where the fluorophores are supposed to be closest and may be due to partial contact quenching.[16]

In extension of this approach we have conducted experiments where the two dyes in the actuator were replaced by an amine group and a carboxylic acid group, respectively. Chemical coupling reactions were performed for each of the 11 different states of the actuator (Figure 3g–i). The chemical reactions lead to cross-linking of the two pistons by amide formation and lead to a 128 nucleotide product clearly seen when analyzed by PAGE. The yields of the chemical reactions are generally low, but the reactions show the same trend as obtained by FRET measurements. Significant amounts of the products are only observed from states where the chemical groups are in proximity (see section S5 in the Supporting Information for detailed conjugation and reaction methods).

In all experiments shown above, each measurement was carried out on separate samples, with the ABR structure and a specific lock. To demonstrate the dynamics of the actuator by the successive switching between specific states, we successively inserted and removed locks L0, L5, and L10 in the same ABR sample. Each lock strand is equipped with a 10 nucleotide toehold region placed at the 3′-end to allow removal of the lock by strand displacement upon addition of a fully complementary unlock strand (LCn). This type of strand displacement is commonly used to switch between states in DNA nanomachines.[9b] The design of the experiment is shown in Figure 4a and native PAGE is used for characterization of this dynamic process (Figure 4b). Initially the ABR actuator is assembled without lock strands (lane 2), then lock L0 is added to lock it in state S0 (lane 3), followed by the addition of the unlock strand LC0, thus resulting in a change in mobility that corresponds to the unlocked ABR actuator (lane 4). This result indicates that the locks are removed and the short waste product of the L0–LC0 hybrid is observed at the bottom of the gel. Subsequently, L5 is added to the sample and leads to a band of lower mobility, thus indicating the formation of the ABR–L5 complex (lane 5). The lock L5 is removed again with the complementary strand LC5 (lane 6), and this switching is continued by adding L10 (lane 7). All steps were performed successively from lanes 2 to 7, which shows that it is possible to remove the lock strands and replace them with others to form stable complexes. The reverse switching from state S10, via state S5 to state S0 was also demonstrated (Figure S11).

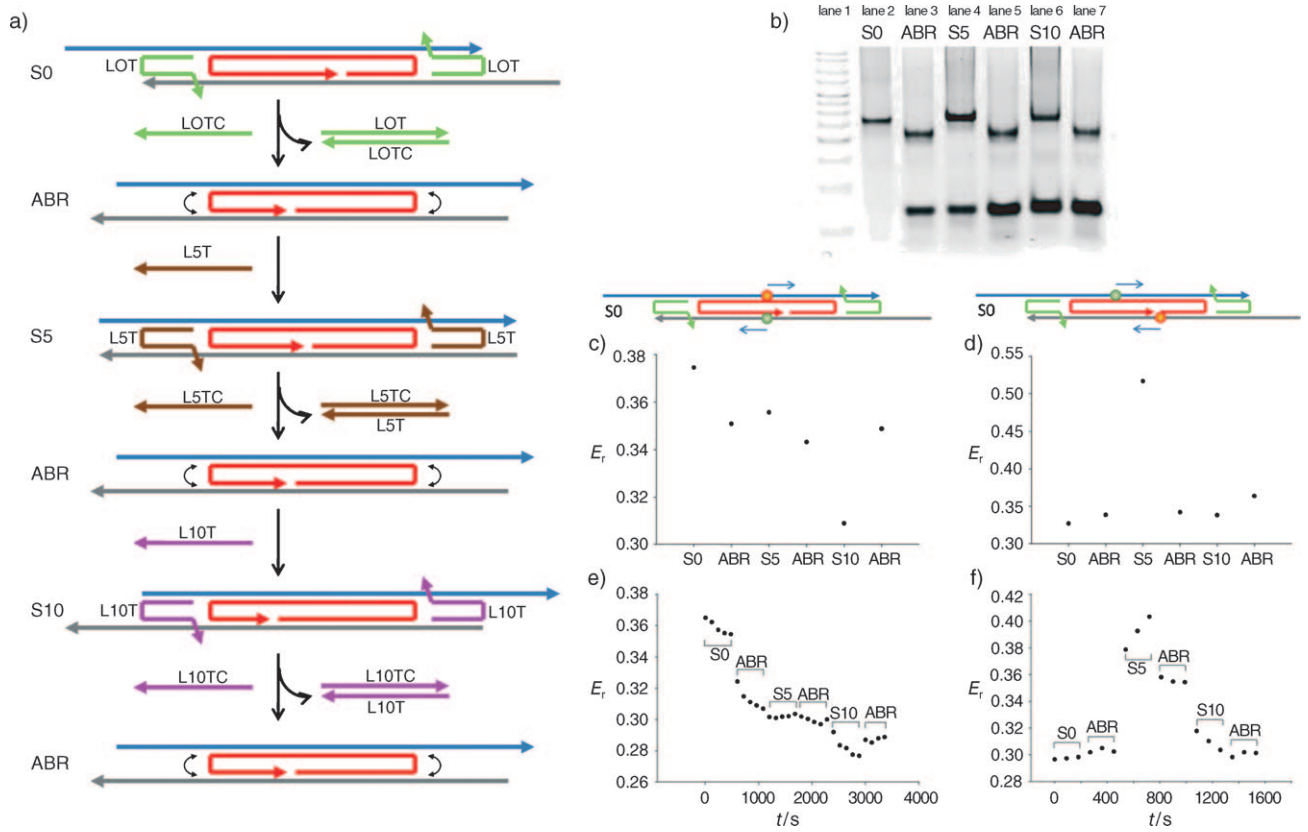

Figure 4. Switching between states of the actuator by inserting and removing lock strands. a) Schematic drawing of the switching between states S0, S5, or S10, by inserting and removing distinct lock strands. A 10 nucleotide toehold at the 3' end of each lock enables strand displacement by fully complementary unlock (LCn) strands. b) Native PAGE (7.5% gel) analysis of consecutive additions of locks and unlocks from S0 to S5 then to S10, after isothermal incubation at 37°C for 20 min in each step. c) Monitoring the switching by FRET on an actuator with Cy3B and Alexa647 dyes located 16 nucleotides from the right-hand half crossover of the roller in S0. d) Similar experiments with the dyes Alexa555 and Alexa647 located 21 and 11 nucleotides from the right-hand half crossover of the roller in S0, e, f) time-resolved FRET experiments where the additions were performed every 600 (e) or 270 s (f).

To verify that the actuator is actually sliding from state to state during the consecutive lock replacements, we have performed the replacement experiments on the actuators presented in Figure 3 where FRET pairs were incorporated (Figure 4c–f). In the first two sets of data we have allowed the actuators to reach equilibrium before the FRET data were recorded. The FRET data obtained from states S0, S5, and S10 correlate very well with the data obtained for the static experiments shown in Figure 3, that is, higher FRET values are obtained when the dyes are closer to each other. Thus we can conclude that the actuator does undergo the predicted sliding during the strand displacements.

The dynamics of the strand replacements and the free actuator motion was further investigated in two time-resolved experiments where the additions of lock and unlock strands were performed every 270 s or 600 s and 3–5 data points were recorded after each addition (Figure 4e,f). The actuator responds to the addition of lock strands to lock the actuator in a specific position and the corresponding change in FRET signal indicates that the locks are pushing the actuator into the locked position.

In spite of its structural simplicity, the actuator presented herein displays a remarkable control of mechanical movement. In a pseudo-one-dimensional sliding motion it can be locked in 11 separate states and move dynamically with a maximal extension of 7.5 nm. The ability to switch from state to state holds promise for application as a nanoscale robot arm. Several actuators may be integrated into larger nanostructures such as DNA origami to regulate the spacing between integrated nano-sized components and it may potentially be used to build complex assembly lines.[3,17] Polymerization of the actuator with a second roller may be used for amplification of the action of a single lock in sensing devices where the target acts as the lock. Polymerized actuators may also be used for the transformation of information given as an input at one end of the polymeric actuator over a relatively long distance to the other end. The actuator presented herein expands the possibilities to design more complex dynamic DNA machines.

Received: December 6, 2010
Published online: March 21, 2011

Keywords: DNA · DNA structures · FRET · molecular devices · nucleic acid hybridization

[1] a) J. Bath, A. J. Turberfield, *Nat. Nanotechnol.* **2007**, *2*, 275 – 284; b) N. C. Seeman, *Mol. Biotechnol.* **2007**, *37*, 246 – 257.

[2] a) C. Mao, W. Sun, Z. Shen, N. C. Seeman, *Nature* **1999**, *397*, 144 – 146; b) H. Yan, X. Zhang, Z. Shen, N. C. Seeman, *Nature* **2002**, *415*, 62 – 65.

[3] H. Gu, J. Chao, S. J. Xiao, N. C. Seeman, *Nature* **2010**, *465*, 202 – 205.

[4] a) L. Feng, S. H. Park, J. H. Reif, H. Yan, *Angew. Chem.* **2003**, *115*, 4478 – 4482; *Angew. Chem. Int. Ed.* **2003**, *42*, 4342 – 4346; b) F. A. Aldaye, H. F. Sleiman, *J. Am. Chem. Soc.* **2007**, *129*, 4130 – 4131; c) F. A. Aldaye, H. F. Sleiman, *J. Am. Chem. Soc.* **2007**, *129*, 13376 – 13377; d) R. P. Goodman, M. Heilemann, S. Doose, C. M. Erben, A. N. Kapanidis, A. J. Turberfield, *Nat. Nanotechnol.* **2008**, *3*, 93 – 96; e) B. Chakraborty, R. Sha, N. C. Seeman, *Proc. Natl. Acad. Sci. USA* **2008**, *105*, 17245 – 17249.

[5] R. Holliday, *Genet. Res.* **1964**, *5*, 282 – 304.

[6] N. R. Kallenbach, R. I. Ma, N. C. Seeman, *Nature* **1983**, *305*, 829 – 831.

[7] a) S. Venkataraman, R. M. Dirks, P. W. Rothemund, E. Winfree, N. A. Pierce, *Nat. Nanotechnol.* **2007**, *2*, 490 – 494; b) J. Bath, S. J. Green, K. E. Allen, A. J. Turberfield, *Small* **2009**, *5*, 1513 – 1516.

[8] a) J. S. Shin, N. A. Pierce, *J. Am. Chem. Soc.* **2004**, *126*, 10834 – 10835; b) T. Omabegho, R. Sha, N. C. Seeman, *Science* **2009**, *324*, 67 – 71; c) W. B. Sherman, N. C. Seeman, *Nano Lett.* **2004**, *4*, 1203 – 1207.

[9] a) R. Chhabra, J. Sharma, Y. Liu, H. Yan, *Nano Lett.* **2006**, *6*, 978 – 983; b) B. Yurke, A. J. Turberfield, A. P. Mills, Jr., F. C. Simmel, J. L. Neumann, *Nature* **2000**, *406*, 605 – 608; c) Y. Tian, C. Mao, *J. Am. Chem. Soc.* **2004**, *126*, 11410 – 11411; d) X. Han, Z. Zhou, F. Yang, Z. Deng, *J. Am. Chem. Soc.* **2008**, *130*, 14414 – 14415.

[10] R. Sha, F. Liu, N. C. Seeman, *Biochemistry* **2000**, *39*, 11514 – 11522.

[11] T. J. Fu, N. C. Seeman, *Biochemistry* **1993**, *32*, 3211 – 3220.

[12] P. W. Rothemund, *Nature* **2006**, *440*, 297 – 302.

[13] E. S. Andersen, M. Dong, M. M. Nielsen, K. Jahn, A. Lind-Thomsen, W. Mamdouh, K. V. Gothelf, F. Besenbacher, J. Kjems, *ACS Nano* **2008**, *2*, 1213 – 1218.

[14] TAE buffer: mixture of tris(hydroxymethyl)aminomethane (Tris base), acetic acid, and ethylenediaminetetraacetic acid (EDTA).

[15] a) R. M. Clegg, *Curr. Opin. Biotechnol.* **1995**, *6*, 103 – 110; b) D. M. J. Lilley, T. J. Wilson, *Curr. Opin. Chem. Biol.* **2000**, *4*, 507 – 517.

[16] a) N. Di Fiori, A. Meller, *Biophys. J.* **2010**, *98*, 2265 – 2272; b) S. A. E. Marras, F. R. Kramer, S. Tyagi, *Nucl. Acids Res.* **2002**, *30*, e122.

[17] Y. He, D. R. Liu, *Nat. Nanotechnol.* **2010**, *5*, 778 – 782.